

Implications of turbulence for jets in core-collapse supernova explosions

Avishai Gilkis¹ and Noam Soker¹

ABSTRACT

We show that turbulence in core collapse supernovae (CCSNe) which has been shown recently to ease shock revival can also lead to the formation of intermittent thick accretion disks, or accretion belts, around the newly born neutron star (NS). The accretion morphology is such that two low density funnels are formed along the polar directions. The disks then are likely to launch jets with a varying axis direction, i.e., jittering-jets, through the two opposite funnels. The energy contribution of jets in this *jittering jets mechanism* can result in an explosion energy of $E_{\text{exp}} \gtrsim 10^{51}$ erg, even without reviving the stalled shock. We strengthen the jittering jets mechanism as a prominent explosion mechanism of CCSNe.

1. INTRODUCTION

Massive stellar cores undergo catastrophic collapse as their final stage of evolution - this collapse is hypothesized to result in energetic, luminous explosions termed core-collapse supernovae (CCSNe). Of the several proposed theoretical explanations for the explosion mechanism (see Janka 2012 for a review), the most prominent are neutrino-driven explosions (Colgate & White 1966) and jet-driven explosions (e.g. LeBlanc & Wilson 1970; Khokhlov et al. 1999; Lazzati et al. 2012). The most modern neutrino-driven model is the thirty-years old so-called delayed-neutrino mechanism (Wilson 1985; Bethe & Wilson 1985), while jet-driven models have reincarnated in the jittering-jets mechanism (Papish & Soker 2011, 2012b, 2014a,b).

In the delayed-neutrino mechanism, neutrinos that are emitted by the newly formed neutron star (NS) within a period of $t \approx 1$ s after the core bounce heat the region below the stalled shock, at $r \approx 100 - 200$ km from the NS. It has been suggested that subsequent neutrino-heating of the gain region will revive the stalled shock, thereby exploding the star with the observed energy of $E_{\text{exp}} \gtrsim 1$ foe, where $1 \text{ foe} \equiv 10^{51}$ erg.

Widely varying outcomes have emerged from increasingly sophisticated multidimensional simulations of the delayed-neutrino mechanism (e.g., Bethe & Wilson 1985; Burrows & Lattimer

¹Department of Physics, Technion – Israel Institute of Technology, Haifa 32000, Israel; agilkis@tx.technion.ac.il; soker@physics.technion.ac.il

1985; Burrows et al. 1995; Fryer & Warren 2002; Buras et al. 2003; Ott et al. 2008; Marek & Janka 2009; Nordhaus et al. 2010; Brandt et al. 2011; Hanke et al. 2012; Kuroda et al. 2012; Hanke et al. 2012; Mueller et al. 2012; Bruenn et al. 2013; Mueller & Janka 2014a; Mezzacappa et al. 2014). Many of these failed to revive the stalled shock while others produced tepid explosions with energies less than 1 foe. In spherically symmetric calculations (1D), the vast majority of progenitors cannot even explode (Burrows et al. 1995; Rampp & Janka 2000; Mezzacappa et al. 2001; Liebendörfer et al. 2005). The explosion of the $8.8M_{\odot}$ progenitor of Nomoto & Hashimoto (1988) in a 1D study with an energy of $\sim 3 \times 10^{49}$ erg is attributed to neutrino-driven wind (Kitaura et al. 2006).

In recent years, the standing accretion-shock instability (SASI; e.g., Blondin et al. 2003; Blondin & Mezzacappa 2007; Fernández 2010) that appears in many two-dimensional axisymmetric calculations (Burrows et al. 1995; Janka & Mueller 1996; Buras et al. 2006a,b; Ott et al. 2008; Marek & Janka 2009) has been studied as a possible driving force for stellar explosions within the delayed-neutrino mechanism (Rantsiou et al. 2011 further suggested the spiral mode of the SASI as the source of pulsar angular momentum). However, recent three dimensional studies gave mixed results (Nordhaus et al. 2010; Janka 2013; Couch 2013; Takiwaki et al. 2014; Dolence et al. 2013; Hanke et al. 2012, 2013; Couch & O’Connor 2014; Mezzacappa et al. 2014). While Nordhaus et al. (2010) and Dolence et al. (2013) found it easier to revive the stalled shock in 3D simulations, most studied have found that explosions are harder to achieve in 3D than 2D (Janka 2013; Couch 2013; Takiwaki et al. 2014; Hanke et al. 2012, 2013; Couch & O’Connor 2014). Most striking is the comparison of the 2D and 3D results of the Oak Ridge group. In their 2D simulations Bruenn et al. (2013, 2014) successfully revived the shock with explosion energy estimates of approximately 0.1 – 0.8 foe. However, in the newer 3D case presented by Mezzacappa et al. (2014) the shock radius position is similar to their results of 1D simulations where no explosion had been obtained. A summary of some of these studies and an account of the seemingly successful explosion of Bruenn et al. (2013) are given by Papish et al. (2015).

Even if the simulations overcome the problem of shock revival, in most cases of unscaled simulations the explosion energy is lower than required – less than 1 foe. Papish & Soker (2012a) and Papish et al. (2015) argued that there is a generic problem of the delayed-neutrino mechanism that prevents it from exploding the star with energies above 5×10^{50} erg, and in most cases much lower.

Recently Couch & Ott (2013), Couch & Ott (2014), and Mueller & Janka (2014b) argued that the effective turbulent ram pressure exerted on the stalled shock allows shock revival with less neutrino heating than 1D models. However, Abdikamalov et al. (2014) found that increasing the numerical resolution allows cascade of turbulent energy to smaller scales, and the shock revival becomes harder to achieve at high numerical resolution. We here nonetheless study the implica-

tion of the turbulence on the stochastic accretion of angular momentum onto the newly formed NS. In section 2 we show implications of accretion of material from a convective region of the progenitor star for formation of intermittent thick disks around the NS, and in section 3 we discuss the implications of accretion of many convective elements simultaneously. In section 4 we briefly discuss the stochastic angular momentum in the post-bounce turbulent core, and summarize.

2. ACCRETION OF ONE CONVECTIVE ELEMENT

2.1. Thin accretion disk

To demonstrate that the turbulent convection required to revive the stalled shock can lead to intermittent disk formation we consider a progenitor with an initial main sequence mass of $M_{\text{ZAMS}} = 15M_{\odot}$ and solar metallicity ($Z = 0.014$). We evolve the star using version 5819 of the Modules for Experiments in Stellar Astrophysics (MESA; Paxton et al. 2011, 2013). Just before core collapse the velocity of convection in the silicon layer, given by the mixing-length theory (MLT) employed by MESA, has a Mach number of $\mathcal{M}_c \approx 0.01$. However, some studies of realistic hydrodynamical simulations of convection in stellar interiors show higher convective velocities of $\mathcal{M}_c \approx 0.1 - 0.2$ (Bazán & Arnett 1998; Asida & Arnett 2000). While recent studies (Couch & Ott 2013, 2014; Mueller & Janka 2014b) have shown that initial conditions motivated by these results alleviate the required neutrino energy for a shock revival in the delayed-neutrino mechanism, we focus on the implications for stochastic angular momentum in the collapsing material, and subsequently the possible formation of accretion disks and jets.

Similarly to Gilkis & Soker (2014), where the details of the calculations can be found, we calculate the variance of the specific angular momentum. We assume a random velocity $\vec{v} = v_c (\sin \theta \cos \varphi, \sin \theta \sin \varphi, \cos \theta)$, where v_c is the convective speed, with a uniform probability density in θ and φ (the angles relative to the z -axis and x -axis, respectively - although the choice of axes is inconsequential). The expectation value for the specific angular momentum along a specific direction, here taken to be the z axis, is zero, while the variance is

$$\text{Var}(j_z) = \langle j_z^2 \rangle = (v_c r_l)^2 \frac{\int [(\hat{r}_l \times \hat{v}(\Omega)) \cdot \hat{z}]^2 d\Omega}{\int d\Omega} = \frac{1}{3} (v_c r_l)^2 \sin^2 \theta_l \quad (1)$$

where r_l is the original location of the convective cell, and θ_l is the positional latitude from the z -axis. Averaging over all possible positions gives

$$\overline{\text{Var}(j_z)} = \frac{\int d\varphi_l \int d\theta_l \sin \theta_l \text{Var}(j_z(\theta_l))}{\int d\Omega_l} = \frac{2}{9} (v_c r_l)^2, \quad (2)$$

which is the same for j_x and j_y . Taking just one component of the angular momentum gives a slight underestimation for its magnitude, but simplifies the derivation here, and more so in the next

section where we calculate the average angular momentum of many cells. The average standard deviation for a single convective element is then

$$\sigma_j \equiv \overline{\sigma(j_z)} = \frac{\sqrt{2}}{3} v_c r_l, \quad (3)$$

where $v_c(r_l)$ is calculated at the original location of the convective element (cell) r_l . The specific angular momentum of a Keplerian orbit at the NS surface is

$$j_{\text{NS}} = \sqrt{GM_{\text{NS}}R_{\text{NS}}}, \quad (4)$$

so that the ratio between the standard deviation of the specific angular momentum of a single convective element (cell) and the minimum required to avoid direct accretion from the equatorial plane is

$$\frac{\sigma_j}{j_{\text{NS}}} \simeq 0.55 \left(\frac{\mathcal{M}_c}{0.1} \right) \left(\frac{c_s}{5000 \text{ km s}^{-1}} \right) \left(\frac{r_l}{5000 \text{ km}} \right) \left(\frac{M_{\text{NS}}}{1.4M_{\odot}} \right)^{-1/2} \left(\frac{R_{\text{NS}}}{25 \text{ km}} \right)^{-1/2}, \quad (5)$$

where c_s is the sound speed given at r_l (the radius of origin of the convective cell), \mathcal{M}_c is the convective Mach number, and typical values for the silicon layer of a pre-collapse core have been inserted. The choice of $R_{\text{NS}} \simeq 25 \text{ km}$ is due to the protoneutron star (PNS) needing to cool down before shrinking to estimated radii of observed neutron stars.

We apply equation (5) to a stellar model of $M_{\text{ZAMS}} = 15M_{\odot}$ that we evolve with MESA just to the point of core collapse. Figure 1 shows that the stochastic deviations of specific angular momentum are close to that of a Keplerian orbit at the NS surface. This means that some fraction of the in-falling material has sufficient specific angular momentum to temporarily form accretion disks around the NS.

2.2. Thick accretion disk

The above derivation is limited to the case of a thin accretion disk - an accretion disk with an opening angle (where there is no gas) from the angular momentum axis of $\theta = 90^\circ$. The inflowing gas is in the equatorial plane, i.e., at latitude of $\theta = 90^\circ$ to the angular momentum axis. If the thick accretion disk is very close to the NS, we can term it an accretion belt. This is likely to be the case, since the intermittent accretion disk will have no time to spread outward. For a thick accretion disk (or a belt) with an opening angle θ (i.e., the surface of the disk is at an angle θ from the angular momentum axis, and the other side at an angle θ from the opposite direction of the axis), the inflowing material on the surface of the disk needs a minimum specific angular momentum of

$$j_{\text{NS}}(\theta) = \sqrt{GM_{\text{NS}}R_{\text{NS}} \sin \theta}, \quad (6)$$

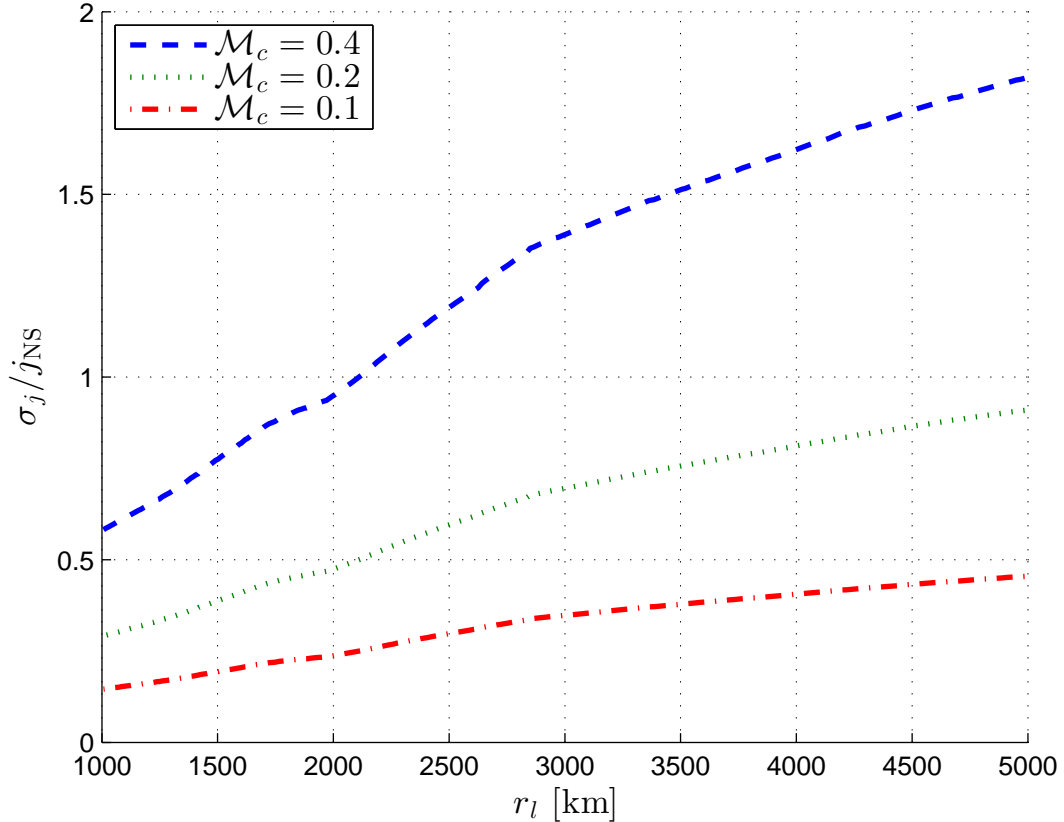


Fig. 1.— Ratio between the standard deviation of the specific angular momentum of a single convective mass element to the specific angular momentum of a Keplerian orbit around a NS with a radius of $R_{\text{NS}} = 25$ km (as given in eq. 5), as function of original radius of in-falling material. The standard deviation is calculated, for our $M_{\text{ZAMS}} = 15M_{\odot}$ stellar model, using the local sound speed $c_s(r_l)$ and for three different Mach numbers (given in the inset) for the convective velocity at the layer of origin of the convective element (r_l). The values close to unity of this ratio imply that some mass elements can form a temporary accretion disk around the newly formed NS.

in order to spiral around the NS surface. It must lose some angular momentum before being accreted; this specific angular momentum is only $\sqrt{\sin \theta}$ times that required for a thin disk. From equation (6) we can estimate the probability for an inflowing parcel of gas to be limited to an angle, from the angular momentum axis, larger than θ_a . As our assumptions constrain the specific angular momentum of the convective elements to $-v_c r_l \leq j_z \leq v_c r_l$, a beta distribution is appropriate,

$$f(j_z) = \frac{\left(\frac{1}{2} + \frac{1}{2} \frac{j_z}{v_c r_l}\right)^{\alpha-1} \left(\frac{1}{2} - \frac{1}{2} \frac{j_z}{v_c r_l}\right)^{\beta-1}}{B(\alpha, \beta)}, \quad (7)$$

where $f(j_z)$ is the probability density function for a convective element to have a specific angular momentum component j_z , α and β are shape parameters determined by the expectation value and variance, and $B(\alpha, \beta)$ is the beta function. An expectation value of zero for j_z and the variance from equation (2) give $\alpha = \beta = 7/4$. The desired probability function is given by

$$\xi(\theta_a) = 2 \int_{j_z = \min(j_{NS} \sin \theta_a, v_c r_l)}^{j_z = v_c r_l} dj_z f(j_z) = 2(1 - I_x(\alpha, \beta)), \quad (8)$$

where $\xi(\theta_a)$ is the probability that accretion of a convective parcel of gas will be limited to an angle of $\pi - \theta_a > \theta > \theta_a$, and $I_x(\alpha, \beta)$ is the regularized incomplete beta function with

$$x = \min\left(\frac{1}{2} + \frac{1}{2} \frac{j_{NS} \sin \theta}{v_c r_l}, 1\right). \quad (9)$$

The factor 2 in front of the integral (possible with the $\alpha = \beta$ symmetry) is for the two sides of the equatorial plane: between θ_a and 90° , and between 90° and $(180^\circ - \theta_a)$.

This probability for a given angle θ_a as function of the radius of origin r_l can be calculated from equations (8) and (9) for a given limiting angle θ_a . We present this in Fig. 2 for the same stellar model used for Fig. 1. To better understand the meaning of $\xi(\theta_a)$ we can examine limiting cases. If there is no stochastic angular momentum at all, i.e., $v_c r_l \ll j_{NS}$, then $\xi = 2(1 - I_1(\alpha, \beta)) = 0$ for all angles. Namely, the probability for limiting the angle is zero as expected since there is no angular momentum and hence each parcel of gas can in principle be accreted from any direction. If the angular momentum fluctuations are huge, $v_c r_l \gg j_{NS}$, then $\xi = 2(1 - I_{1/2}(\alpha, \beta)) = 1$. Namely, for all angles the probability for accretion above the angle is 1, and hence below the angle is zero. This is true even for $\theta = 90^\circ$, which implies that the accreted gas is stopped from inflowing due to a centrifugal barrier at radii larger than the NS radius. Further angular momentum loss in a viscous disk will allow accretion. Other examples are in the caption of Fig. 2.

3. ACCRETION OF MULTIPLE CONVECTIVE ELEMENTS

The accretion of material from a single convective element is a simplified case, as in reality many elements with close radii of origin may undergo accretion at overlapping times. For simul-

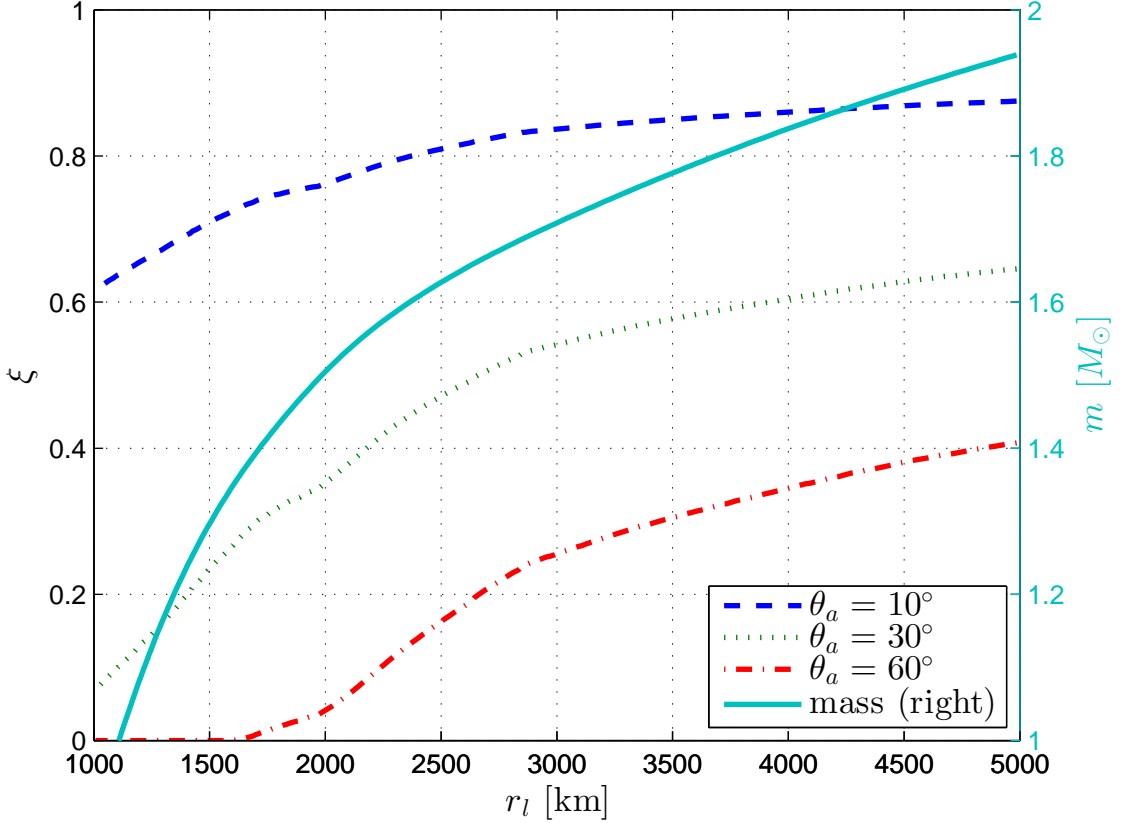


Fig. 2.— The probability for accretion onto the NS to be limited to an angle $\theta > \theta_a$ as a function of radius of origin of the convective mass element in the core, and for three values of the angle from the angular momentum axis θ_a (given in the inset). This is calculated for a convective Mach number of $\mathcal{M}_c = 0.2$ and assuming a beta distribution (eq. 7). For example, material falling from $r_l = 4000$ km has a 60% probability of having a specific angular momentum limiting the accretion to take place from an angle larger than 30° from the angular momentum axis. Limitation to $\theta > \theta_a = 0$ (all lines on the $\xi = 0$) would imply a spherical accretion flow, since all angles are allowed – this is the case when there is not no stochastic motion at the shell of origin of the inflowing gas. On the other hand, a value of $\xi = 1$ for all angles θ_a implies that the gas has a specific angular momentum too high to be directly accreted onto the NS. A thin accretion disk will be formed, and accretion will proceed by angular momentum loss in the disk. Values of $\xi > 0$ lead to the formation of a low density accretion funnel along the angular momentum axis. The solid line shows the inwards baryonic mass at each radius of the pre-collapse core (refers to the right axis).

taneous accretion of multiple convective elements (which we assume to have equal masses), with stochastically varying velocities, the variance of the specific angular momentum becomes

$$\text{Var}(j_{z,N}) = \frac{2}{9N}(\mathcal{M}_c c_s r_l)^2, \quad (10)$$

where N is the number of convective elements in the shell from which the mass is accreted at the given specific time, and \mathcal{M}_c is the Mach number of the convective cells. This is equation (2) with a factor of N^{-1} and with $\mathcal{M}_c c_s = v_c$. We get a narrower distribution of the angular momentum for $N > 1$; for the beta distribution we assumed in the previous section we get

$$\alpha = \beta = \frac{9N}{4} - \frac{1}{2}. \quad (11)$$

The number N can be estimated using the mixing-length (which is proportional to the pressure scale-height) or from the relevant mode order, such as those used by Couch & Ott (2013, 2014) or Mueller & Janka (2014b). For example, Couch & Ott (2013) use sinusoidal perturbations (their eq. 1) which directly give us the number of elements in a shell. For example, their equation (1) would give for $n = 3$ and $n = 5$ modes a total of $N = 12$ and $N = 40$, respectively. A rough estimation using MLT, taking spherical elements with size $r_{\text{elem}} = \alpha_{\text{MLT}} H_P$ (α_{MLT} being the MLT parameter and H_P the pressure scale height) so that

$$N \approx \frac{4\pi r_l^2}{\pi r_{\text{elem}}^2}, \quad (12)$$

gives values of $N \approx 20 - 40$ for the region of interest.

As we consider non-rotating stars, the total angular momentum is zero. We consider fluctuations in angular momentum, but not only within a shell, but also between shells. When a shell has (temporarily) non-zero angular momentum, other shells will compensate with angular momentum axes with other orientations, for a total of zero angular momentum. Over time an exchange of angular momentum takes place between shells (as well as between convective elements). Even for rotating stars, convective regions may give rise to temporary deviations from the angular momentum dictated by the rotation (hence leading to jittering jets). It is important to note that Couch & Ott (2013, 2014) and Mueller & Janka (2014b) considered only fluctuations within each shell, but the sum of angular momentum was zero in each shell. This might explain why they did not get accretion belts.

As shown in Fig. 3, the inclusion of several convective elements results in smaller opening angles (thicker disks) for the thick disk than in the single parcel presented in Fig. 2. As the convective region is turbulent and disorderly, this picture of symmetric accretion is not an accurate description. The accretion process will be something between the parameters of Fig. 2 and those in Fig. 3.

The meaning of figure 3 is as follows. If there was no turbulence at all, then all lines would be on the $\xi = 0$ axis, implying that angular momentum does not prevent any gas from being accreted from all angles. However, the turbulence and the resulting stochastic angular momentum of the accreted mass imply that a substantial fraction of the mass is prevented from being accreted from a direction close to the angular momentum axis (on both opposite sides of the angular momentum axis). Figure 3 shows, for example, that for mass originating at $r_l = 2000$ km, on average 20% of the mass cannot be accreted at all from within an angle of 10° from the angular momentum axis because of a centrifugal barrier. The outcome is the formation of two low-density opposite funnels of the in-falling gas along the angular momentum axis. Due to the stochastic nature, the angular momentum axis is not a constant axis, but rather varies with time; i.e., it jitters.

4. DISCUSSION AND SUMMARY

We have studied the formation of intermittent accretion disks by the collapsing convective regions of the core in core collapse supernovae (CCSNe). This study is motivated by the usage of convective core regions, which might be more vigorous than what the mixing length theory (MLT) gives (e.g., Arnett et al. 2009, Viallet et al. 2013), to facilitate the revival of the stalled shock (Couch & Ott 2013, 2014; Mueller & Janka 2014b). Even if the stalled shock in CCSNe is revived, the desired explosion energy of $E_{\text{exp}} \gtrsim 10^{51}$ erg is unlikely to be achieved (Papish et al. 2015). The convective regions on the other hand are likely to lead to the formation of intermittent accretion disks that can launch jets (Gilkis & Soker 2014) that are more likely to explode the star than the revival of the stalled shock can (Papish & Soker 2014a,b).

We here extended our earlier study (Gilkis & Soker 2014) in discussing the formation of a thick accretion disk (or an accretion belt), and not only a thin accretion disk, and in referring specifically to the convection topology used by Couch & Ott (2013), Couch & Ott (2014), and Mueller & Janka (2014b). The ordered structure introduced in these previous works (with zero angular momentum in each shell) is not representative of the turbulent flow structure. It likely overlooks the possibility of angular momentum deviations between shells. We considered fluctuations of angular momentum between shells, not only within shells. We found that these between-shells angular momentum fluctuations can lead to intermittent thick accretion disk (belt) formation.

As evident from Fig. 3 the accretion from such a convective region forms an accretion belt (or a thick accretion disk) that leaves a funnel along the polar directions. The general accretion flow not only leaves two opposite funnels of a very low density, but around the funnels the gas is rapidly rotating. The turbulent accretion belt is very likely to amplify magnetic fields. This is similar to the finding of Masada et al. (2014) of the development of turbulence and magnetic field amplification around a nascent proto-NS. The funnel, rotation, and magnetic field amplification

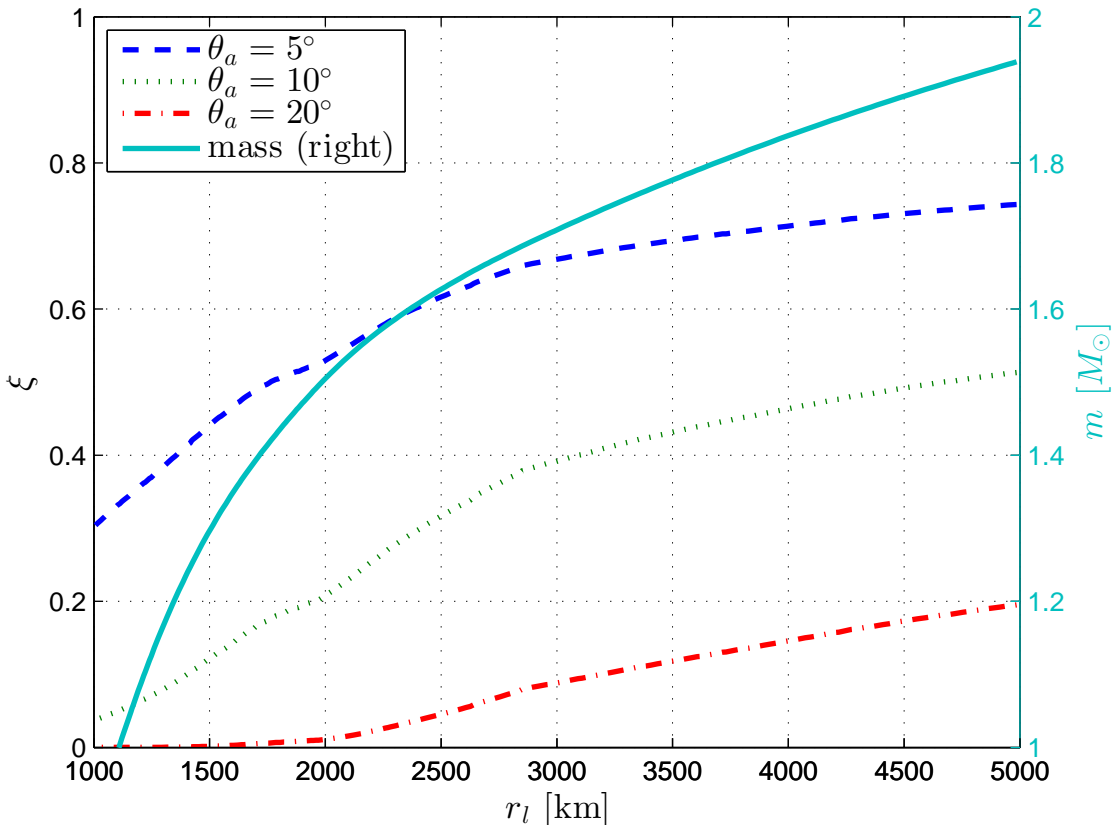


Fig. 3.— Same as Fig. 2 but for accretion of a shell with an $n = 3$ mode (shell with $N = 12$ “blobs”) using eq. (1) of Couch & Ott (2013), and for different limiting angles. For example, about 40% of the accreted mass from a shell starting at $r_l = 3000$ km will not be allowed to be accreted within 10° from the angular momentum axis (intersection of the the blue dashed line with the $r_l = 3000$ km line), and 9% of the mass starting at the same shell will not be able to be accreted from within 20° from the angular momentum axis (intersection of the green dotted line with the $r_l = 3000$ km line). The implication is that a low density funnel is formed along the two opposite sides of the axis.

are the ingredients that very likely form jets. The formation of such jets is along the jittering-jets scenario (Papish & Soker 2014a,b).

There are some difficulties in relating the stochastic angular momentum, clearly present in the convective region prior to collapse, to the angular momentum of material reaching the newly-formed compact object. This is because the accreted gas goes through the shock wave moving through the turbulent region from the shock down to the newly born neutron star (NS) or black hole (BH). The turbulent region between the stalled shock and down to the newly born NS or BH might increase or decrease the variance of the specific angular momentum. Multidimensional hydrodynamic simulations are required to resolve this question. We here try to estimate the stochastic specific angular momentum from existing simulations.

Recent studies (e.g., Couch & Ott 2014) have focused on the turbulent energy in the gain region, giving typical values for the mass M_{turb} and energy E_{turb} in this turbulent region. We take

$$\overline{v_{\text{turb}}} \equiv \sqrt{\frac{2E_{\text{turb}}}{M_{\text{turb}}}}, \quad (13)$$

use equation (3) to approximate $j_{\text{turb}} \approx \sigma_j = \frac{\sqrt{2}}{3} \overline{v_{\text{turb}}} r_l$, and substitute typical values to derive

$$\frac{j_{\text{turb}}}{j_{\text{NS}}} \approx 0.2 \left(\frac{E_{\text{turb}}}{2 \times 10^{49} \text{ erg}} \right)^{1/2} \left(\frac{M_{\text{turb}}}{0.05 M_{\odot}} \right)^{-1/2} \left(\frac{r_l}{150 \text{ km}} \right) \left(\frac{M_{\text{NS}}}{1.4 M_{\odot}} \right)^{-1/2} \left(\frac{R_{\text{NS}}}{25 \text{ km}} \right)^{-1/2}. \quad (14)$$

This is valid for symmetric as well as turbulent initial conditions, as turbulence around the NS arises either way (e.g., Mueller & Janka 2014b). Comparing equation (14) with equation (5) with the aid of equation (10), we find that the case given by equation (14) corresponds to a total number of convective cells in the accreted layer of $N \approx 7 - 8$. This will give funnels similar (and even somewhat larger) than those depicted in figure 3 which is given for $N = 12$. This crude estimate suggests that the passage of the material through the stalled shock does not reduce much the stochastic behavior of the angular momentum.

We summarize by restating our main finding that the pre-collapse turbulence structures introduced by Couch & Ott (2013, 2014) and Mueller & Janka (2014b) most likely lead to the formation of intermittent accretion disks. These in turn are likely to launch jets that play a much more important role in exploding the star than the extra pressure of the turbulent motion on the stalled shock region.

This research was supported by the Asher Fund for Space Research at the Technion.

REFERENCES

- Abdikamalov, E., Ott, C. D., Radice, D., et al. 2014, arXiv:1409.7078
- Arnett, D. and Meakin, C., & Young, P. A. 2009, ApJ, 690, 1715
- Asida, S. & Arnett, D. 2000, ApJ, 545, 435
- Bazán, G. & Arnett, D. 1998, ApJ, 496, 316
- Bethe, H. A., & Wilson, J. R. 1985, ApJ, 295, 14
- Blondin, J. M., Mezzacappa, A., & DeMarino, C. 2003, ApJ, 584, 971
- Blondin, J. M., & Mezzacappa, A. 2007, Nature, 445, 58
- Brandt, T. D., Burrows, A., Ott, C. D., & Livne, E. 2011, ApJ, 728, 8
- Bruenn, S. W., Lentz, E. J., Hix, W. R., et al. 2014, arXiv:1409.5779
- Bruenn, S. W., Mezzacappa, A., Hix, W. R., et al. 2013, ApJ, 767, L6
- Buras, R., Rampp, M., Janka, H.-T., & Kifonidis, K. 2003, Physical Review Letters, 90, 241101
- Buras, R., Rampp, M., Janka, H.-T., & Kifonidis, K. 2006, A&A, 447, 1049
- Buras, R., Janka, H.-T., Rampp, M., & Kifonidis, K. 2006, A&A, 457, 281
- Burrows, A., & Lattimer, J. M. 1985, ApJ, 299, L19
- Burrows, A., Hayes, J., & Fryxell, B. A. 1995, ApJ, 450, 830
- Colgate, S. A., & White, R. H. 1966, ApJ, 143, 626
- Couch, S. M. 2013, ApJ, 775, 35
- Couch, S. M., & Ott, C. D. 2013, ApJ, 778, L7
- Couch, S. M., & Ott, C. D. 2014, arXiv:1408.1399
- Couch, S. M., & O’Connor, E. P. 2014, ApJ, 785, 123
- Dolence, J. C., Burrows, A., Murphy, J. W., & Nordhaus, J. 2013, ApJ, 765, 110
- Fernández, R. 2010, ApJ, 725, 1563
- Fryer, C. L., & Warren, M. S. 2002, ApJ, 574, L65

- Gilkis, A. & Soker, N. 2014, MNRAS, 439, 4011
- Hanke, F., Marek, A., Müller, B., & Janka, H.-T. 2012, ApJ, 755, 138
- Hanke, F., Mueller, B., Wongwathanarat, A., Marek, A., & Janka, H.-T. 2013, ApJ, 770, 66
- Janka, H.-T., & Mueller, E. 1996, A&A, 306, 167
- Janka, H.-T. 2012, Annual Review of Nuclear and Particle Science, 62, 407
- Janka H.-T. et al., 2013, Proc. Fifty-one Erg Meeting, available at:
<http://grb.physics.ncsu.edu/FOE2013/WEB/abstracts.html>
- Khokhlov, A. M., Höflich, P. A., Oran, E. S., et al. 1999, ApJ, 524, L107
- Kitaura, F. S., Janka, H.-T., & Hillebrandt, W. 2006, A&A, 450, 345
- Kuroda, T., Kotake, K., & Takiwaki, T. 2012, ApJ, 755, 11
- Lazzati, D., Morsony, B. J., Blackwell, C. H., & Begelman, M. C. 2012, ApJ, 750, 68
- LeBlanc, J. M., & Wilson, J. R. 1970, ApJ, 161, 541
- Liebendörfer, M., Rampp, M., Janka, H.-T., & Mezzacappa, A. 2005, ApJ, 620, 840
- Marek, A., & Janka, H.-T. 2009, ApJ, 694, 664
- Masada, Y., Takiwaki, T., & Kotake, K. 2014, ApJ, in press (arXiv:1411.6705)
- Mezzacappa, A., Liebendörfer, M., Messer, O. E., et al. 2001, Physical Review Letters, 86, 1935
- Mezzacappa, A., Bruenn, S. W., Lentz, E. J., et al. 2014, Astronomical Society of the Pacific Conference Series, 488, 102
- Mueller, B., & Janka, H.-T. 2014a, ApJ, 788, 82
- Mueller, B., & Janka, H.-T. 2014b, arXiv:1409.4783
- Mueller, B., Janka, H.-T., & Marek, A. 2012, ApJ, 756, 84
- Nomoto, K., & Hashimoto, M. 1988, Phys. Rep., 163, 13
- Nordhaus, J., Burrows, A., Almgren, A., & Bell, J. 2010, ApJ, 720, 694
- Ott, C. D., Burrows, A., Dessart, L., & Livne, E. 2008, ApJ, 685, 1069
- Papish, O., Nordhaus, J., & Soker, N. 2015, arXiv:1402.4362

- Papish, O., & Soker, N. 2011, MNRAS, 416, 1697
- Papish, O., & Soker, N. 2012a, Death of Massive Stars: Supernovae and Gamma-Ray Bursts, 279, 377
- Papish, O., & Soker, N. 2012b, MNRAS, 421, 2763
- Papish, O., & Soker, N. 2014a, MNRAS, 443, 664
- Papish, O., & Soker, N. 2014b, MNRAS, 438, 1027
- Paxton, B., Bildsten, L., Dotter, A., et al. 2011, ApJS, 192, 3
- Paxton, B. et al. 2013, ApJS, 208, 4P
- Rampp, M., & Janka, H.-T. 2000, ApJ, 539, L33
- Rantsiou, E., Burrows, A., Nordhaus, J., & Almgren, A. 2011, ApJ, 732, 57
- Takiwaki, T., Kotake, K., & Suwa, Y. 2014, ApJ, 786, 83
- Viallet, M. and Meakin, C. and Arnett, D. & Mocák, M. 2013, ApJ, 769, 1
- Wilson, J. R. 1985, Numerical Astrophysics, 422